 doi:10.20944/preprints202205.0348.v1

Article

Influence of the surface chemistry differences between zirconia and titanium with the same surface topographies on bone formation

Yoshiki TOKUNAGA [1,*], Masatsugu HIROTA [2] and Tohru HAYAKAWA [1]

[1] Department of Dental Engineering, Tsurumi University School of Dental Medicine, 2-1-3 Tsurumi, Tsurumi-ku, Yokohama, Kanagawa 230-8501, Japan; tokunaga-y@tsurumi-u.ac.jp; hayakawa-t@tsurumi-u.ac.jp
[2] Department of Education for Dental Medicine, Tsurumi University School of Dental Medicine, 2-1-3 Tsurumi, Tsurumi-ku, Yokohama, Kanagawa 230-8501, Japan; hirota-masatsugu@tsurumi-u.ac.jp
* Correspondence: tokunaga-y@tsurumi-u.ac.jp; Tel.+81-45-580-8369

Abstract: In previous studies regarding the osseointegration of zirconia (ZrO_2) implants, a lack of consistency was observed in the surface topographies of the ZrO_2 and Ti samples because of the difficult processability of ZrO_2 surfaces. To resolve this problem, we used the molecular precursor method (wet process), which is a surface-modifying technique that can easily change the surface chemistry without changing the surface topography. A roughened Ti surface was prepared using sandblasting (large-grit) and acid treatment. We were able to create ZrO_2-coated Ti implants with the same topography as that of roughened Ti substrates using the molecular precursor method, which solution contained a Zr complex. The uniform presence of tetragonal Zr was confirmed, and the apparent zeta potential of the surface of the ZrO_2-coated Ti implant was higher than that of Ti. In animal experiments, ZrO_2-coated Ti implants showed an equivalent or higher bone-to-implant contact ratio compared to that of the non-coated implants inserted into the femur bone defects of the rats. ZrO_2 with the same surface topography as that of roughened Ti exhibits a promotion of osteogenesis equivalent to or better than that of Ti in the early stages of bone formation.

Keywords: zirconia; molecular precursor method; dental-implant; osseointegration; bone-to-implant contact.

1. Introduction

Using titanium (Ti) as a dental implant material has advantages owing to its excellent mechanical properties and biocompatibility. The tight bonding of the Ti implant to the bone tissue is known as osseointegration. However, the silver color of Ti causes problems with aesthetics. Allergies and hypersensitive reactions to Ti implants have also been reported [1–3]. Recently, a yttria-stabilized tetragonal zirconia polycrystal (Y-TZP) was used as an alternative material to Ti [4]. However, the osseointegration of zirconia (ZrO_2) implants is controversial and its mechanism remains unclear. Kohal et al [5]. evaluated the clinical and radiographic outcomes of 65 one-piece ZrO_2 implants incorporated in humans for three years post operation. The survival rates of zirconia implants were inferior to those of Ti implants with similar shapes. In contrast, Roehling et al [6]. studied 2758 publications in which ZrO_2 and Ti implants were compared and reported that ZrO_2 and Ti implants showed similar soft and hard tissue integration capacities. The research majorly suggested favorable results for ZrO_2 implants in terms of bone adaptation. However, clear evidence of ZrO_2 osseointegration is still scarce.

It is well known that surface topography is key to the osseointegration of dental implants [7]. The surface treatment of Ti implants by combining the large-grit and acid-etched procedures, which is generally named SLA, produced positive effects on the activation of blood platelets and cell migration [8]. The clinical success rate of SLA-Ti implants is approximately 95% [9–11]. The large-grit and acid etching procedures were also applied

Preprints (www.preprints.org) | NOT PEER-REVIEWED | Posted: 25 May 2022 doi:10.20944/preprints202205.0348.v1

to Y-TZP implants, and the effectiveness of these procedures for osteoblast activities and bone response was reported [12]. However, Y-TZP is known to exhibit high strength and chemical stability [13], and achieving the same surface topography on Y-TZP as that on Ti is difficult. Bormann et al [14]. compared the bone tissue response to those of the micro-structured ZrO_2 and SLA-Ti implants. ZrO_2 implants were chemically treated with a hot solution of hydrofluoric acid. They reported that the mean roughness of the SLA-Ti implants (Sa = 1.19 μm) was approximately twice that of similar ZrO_2 implants (Sa = 0.63 μm).

Apart from surface roughness, surface chemistry also affects the osseointegration of dental implants. It is not clear which factor, surface roughness or chemistry, of ZrO_2 implants will contribute more to osseointegration. It is presumed that this is the reason for the controversy regarding the osseointegration of ZrO_2. To elucidate the osseointegration of ZrO_2 implants, it is important to evaluate the bone response of the ZrO_2 surface for the same topography as that of Ti. If we can prepare a ZrO_2 surface with the same topography as that of Ti, we can say something about the contribution of the surface chemistry of ZrO_2 to the osseointegration.

The molecular precursor method is a surface modifying method, i.e., an arbitrary metal oxide film coating on the ceramic and metal surfaces achieved using a metal complex liquid [15–17]. It is a simple and inexpensive technique for preparing metal oxide thin films, such as TiO_2, Co_3O_4, and $SrTiO_3$ [18]. A thin apatite film can be deposited onto the Ti and ZrO_2 surfaces using the Ca–EDTA complex precursor solution [19]. The thickness of the thin apatite film was in the range of 0.6–0.8 μm. The molecular precursor method is a wet process, which can deposit a thin film on three-dimensional fiber structures [20]. Moreover, it should be noted that the molecular precursor method can only change the chemical composition of substrates without changing the surface topography. A thin ZrO_2 film can be deposited on the Ti surface using the Zr-complex precursor solution. Therefore, we can achieve the same surface topography of the ZrO_2 thin film. In other words, the surface topography of ZrO_2 coated on the SLA-Ti surface can be maintained using a molecular precursor method.

In this study, we tried to distinguish the effects of the surface chemistry from those of the surface topography between ZrO_2 and Ti in the osseointegration process. The ZrO_2 coating fabricated by the molecular precursor method changed the chemical composition without changing the surface topography of SLA-Ti. The main purpose of this study is to reveal the effects of the difference in surface chemistry on the bone response with respect to ZrO_2 and Ti with the same surface topography.

2. Materials and Methods

2.1. Specimen preparation and characterization

2.1.1. Fabrication of the roughened Ti surface

Two shapes of Ti samples, disks (12.0 mm in diameter and 1.0 mm in thickness, JIS2 type, 99.9% mass, Furuuchi Chemical Corp., Tokyo, Japan) and rectangular plates (2.0 × 3.0 × 1.0 mm, JIS2 type, 99.9% mass, Furuuchi Chemical Corp., Tokyo, Japan), were used in this study. The surfaces of the specimens were polished with a #1200 waterproof paper under running water. After polishing, the specimens were subjected to SLA treatment. Namely, sandblasting was performed perpendicular to the titanium surface from a distance of 20 mm with 180 μm alumina particles at a 0.6 MPa air pressure. Then, acid etching was performed on the blasted surface with a mixture of 36% hydrochloric acid (HCL) and a 96% sulfuric acid (H_2SO_4) solution for 3 min at 70 °C [21]. SLA-treated specimens were then cleaned in ethanol and distilled water for 20 min using an ultrasonic cleaner (VS-100III; AS ONE Co., Osaka, Japan). Disk specimens were used for the characterization of the ZrO_2 coating and the *in vitro* immersion experiments in phosphate-buffered saline (PBS) and simulated body fluid (SBF). The rectangular plate specimens were used for animal experiments.

Preprints (www.preprints.org) | NOT PEER-REVIEWED | Posted: 25 May 2022 doi:10.20944/preprints202205.0348.v1

2.1.2. ZrO_2 coating using the molecular precursor method

Ti disks and rectangular plates were coated with ZrO_2 (ZrO_2/Ti) using the molecular precursor method. A molecular precursor solution (25 mL) for the ZrO_2 film (Zr complex ethanol solution; Zr ion concentration = 0.32 mmol/g; TFTECH Co. Ltd., Tokyo) was poured on the Ti surface. It was then spin-coated using a spin coater (1H-D7; MIKASA, Tokyo, Japan) in the double step mode at 500 rpm for 5 s and 2000 rpm for 30 s. Ti disks and rectangular specimens covered with precursor films were then heated at 550 °C in air for 30 min using a tubular furnace (EPKPO12-K; ISUZU, Niigata, Japan). A thin film coating of ZrO_2 can be achieved on Ti disks and rectangular plates using this method.

2.1.3. Surface characterization of the ZrO_2 coating

The surface morphology of ZrO_2/Ti was observed using scanning electron microscopy (SEM; SU1510; Hitachi High-Technologies Corp., Tokyo, Japan). The specimens were sputter-coated with Au and observed at an accelerating voltage of 15 kV.

The three-dimensional surface topography of ZrO_2/Ti was observed using atomic force microscopy (AFM; Nanosurf Easyscan 2, Nanosurf AG; Gräubernstras, Switzerland) in the tapping mode (cantilever: TapAl-G; Budget sensors, Bulgaria; resonance frequency = 190 kHz, spring constant = 48 N/m). The average arithmetic roughness of the three-dimensional surface (Sa) was calculated within the 1.0 μm × 1.0 μm, 2.5 μm × 2.5 μm, 5.0 μm × 5.0 μm, and 10.0 μm × 10.0 μm areas of the AFM images. The surface of roughened Ti was also observed using SEM and AFM by the same method. Four measurements were performed on each specimen.

2.1.4. Crystal structure and composition of the ZrO_2 thin film

The crystal structure of the coated ZrO_2 thin film on Ti disks was characterized using X-ray diffraction (XRD; SmartLab; Rigaku, Tokyo, Japan), with a thin layer attachment (incidence angle θ = 0.3°), which had an X-ray source of Cu Kα and a power of 45 kV × 200 mA. The presence of Ti or Zr atoms on Ti and ZrO_2/Ti disks on each surface were confirmed using an electron probe micro analyzer (EPMA; JXA-8900R; JEOL, Tokyo, Japan) at an accelerating voltage of 15 kV. Cross sectional observation was also performed. The disks were then embedded in an epoxy resin. After curing the resin, the specimens were vertically cut through the middle using a cutting machine.

The atom elements in the surface of Ti and Zr/O2 Ti were analyzed by using X-ray photoelectron spectroscopy (XPS; AXIS-ULTRA; Kratos Analytical, England), with an X-ray source of Al Kα and a power of 15 kV × 10 mA.

2.1.5. Apparent zeta potential measurements

Ti plates with dimensions of 1 mm × 10 mm × 20 mm (JIS2 type, 99.9% mass, Furuuchi Chemical Corp., Tokyo, Japan) were prepared as the specimens. The apparent zeta potentials for the solid surfaces of Ti and ZrO_2/Ti plates were monitored with a SurPASS 3 electro-kinetic instrument (Anton Paar GmbH, Graz, Austria). The zeta potential indicates the electrical charging behavior of the material surface. For determining the zeta potential, an aqueous electrolyte solution (1.0 mM of KCl) was used at a pH level of 5.6. The electrolyte solution passed through a thin slit channel formed by two identical sample surfaces. The streaming current and potential resulting from the pressure-driven flow of the electrolyte were measured. The zeta potential was then calculated using the Helmholtz–Smoluchowski equation [22–23]. Furthermore, the pH-dependent curves of the zeta potential were plotted by measuring the zeta potential at any pH level adjusted by 0.05 M HCl and 0.1 M KOH. The isoelectric points of Ti and ZrO_2/Ti were obtained from these curves.

2.1.6. ZrO_2 coating durability

ZrO_2/Ti disks were immersed in 20 mL of a PBS solution (pH = 7.4) in a polypropylene bottle for 90 days. After immersion, the specimens were dried in a desiccator. The

Preprints (www.preprints.org) | NOT PEER-REVIEWED | Posted: 25 May 2022 doi:10.20944/preprints202205.0348.v1

morphological changes in ZrO_2 films were observed using SEM at an accelerating voltage of 15 kV after sputter-coating with Au.

2.2. In vitro biocompatibility evaluation by SBF immersion

Hanks' balanced salt solution (HBSS) without organic species was prepared as an SBF [24]. Ti and ZrO_2/Ti disks were immersed in 20 mL of HBSS with an adjusted pH level of 7.4 at 37 °C in a polypropylene bottle. After immersing for 6 and 24 h, the excess HBSS on the disks was removed using a soft paper, and the disks were immediately dried in a desiccator. The surfaces of the Ti and ZrO_2/Ti disks were then observed using SEM at an accelerating voltage of 15 kV after sputter-coating with Au. The crystallographic structures of the precipitates on the Ti and ZrO_2/Ti disks were analyzed using XRD (RINT-RAPID2 MM007; Rigaku, Tokyo, Japan), with an X-ray source of Cu-Ka at a power of 40 kV × 30 mA, and FT-IR (FT/IR-430; Jasco, Tokyo, Japan) using the KBr method. The precipitated products were detached from the Ti and ZrO_2/Ti disks for FT-IR measurements.

2.3. In vivo study

2.3.1. Animal experiment

The animal experiment was approved by the Animal Experimental Ethical Guidelines of the Tsurumi University, School of Dental Medicine (certificate nos. 19A042, 20A001, and 21A009). Overall, 12 male Wistar rats, each weighing approximately 180 g at 6 weeks of age, were employed. The rats were housed in pairs of two per cage at 20–25 °C in a 12 h circadian light rhythm environment and fed water and food *ad libitum* during the experiment.

Each implant was placed in a femur bone defect [25], and each rat received one implant. Overall, 3 ZrO_2/Ti and 3 Ti implants were inserted for 2- and 4-week implantation periods, respectively.

The surgery was performed under general inhalation anesthesia using a 3% isoflurane and oxygen mixture, which was reduced to 2% isoflurane during surgical manipulation. After shaving the hind limb and disinfecting the operating field, xylocaine was injected as local anesthesia. A longitudinal incision was made on the distal surface of the hind limb to expose the femur. A cortical bone defect measuring 1 mm × 2 mm was created through the cortex and the medulla. The bone defect was prepared using a very gentle surgical technique and continuous internal cooling with a physiological saline solution. After press-fitting an implant into the bone defect, the muscle tissue and skin were closed in separate layers using non-absorbable sutures. After surgery, the rats were injected subcutaneously with benzyl penicillin G procaine (3,000,000 U/kg).

The rats were sacrificed at 2 and 4 weeks after implantation using carbon dioxide gas to harvest the implants and the surrounding femoral bone.

2.3.2. Histological and histomorphometrical observations

After removing the surrounding tissue, the specimens were placed in a 10% neutral buffered formalin solution (pH 7.4), dehydrated through a graded series of ethanol, and embedded in methyl methacrylate. Non-decalcified thin sections with thicknesses of approximately 50–70 μm were created in a direction perpendicular to the axis of the implants using a cutting–grinding technique (EXAKT-Cutting Grinding System, BS-300CP band, system & 400 CS microgrinding system; EXAKT Co., Norderstedt, Germany).

The sections were then stained with methylene blue and basic fuchsin and histologically evaluated using a light microscope (Eclipse N*i*, Nikon Co. Ltd., Tokyo, Japan, magnifications of ×40 and ×100). Additionally, a descriptive evaluation and histomorphometrical analysis were performed. The bone-to-implant contact (BIC) ratio and the bone mass (BM) around the implant were measured using an image analysis system. The BIC ratio was calculated as the percentage of the length of bone-implant contact within the regions of interest (ROI). BM was defined as the percentage of newly formed bone within the ROI. The ROIs for quantitative analysis were determined by following a previous study [26],

Preprints (www.preprints.org) | NOT PEER-REVIEWED | Posted: 25 May 2022 doi:10.20944/preprints202205.0348.v1

as illustrated in Figure 1. The BIC ratio and BM values were determined using an image analysis system (WinROOF, Visual System Division Mitani Corp., Tokyo, Japan).

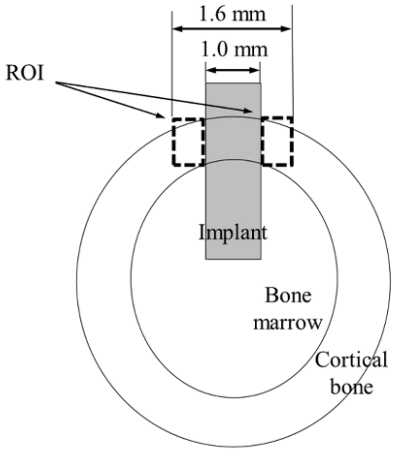

Figure 1. Schematic of the ROI.

2.3.3. Statistical analysis

All data were calculated with the help of SPSS for Windows (SPSS Statics 17.0; SPSS, Chicago, USA). The results of the surface roughness from AFM measurements were compared using the student *t* test. A P value < 0.05 was considered to be significant. The results of the BIC ratio and BM values from histomorphometrical measurements were evaluated by one-way analysis of variance (ANOVA) and the Tukey's test for multiple comparisons among the means at $P = 0.05$.

3. Results

3.1. Surface characterization

3.1.1. Surface morphology and roughness

Figure 2 shows the SEM profiles of the Ti and ZrO_2/Ti disk surfaces. No difference was observed in the surface shapes between the Ti and ZrO_2/Ti disks. Both surfaces had fractal structures, which were formed by irregular roughness. Additionally, the detachment and defect of the ZrO_2 coating film were not observed.

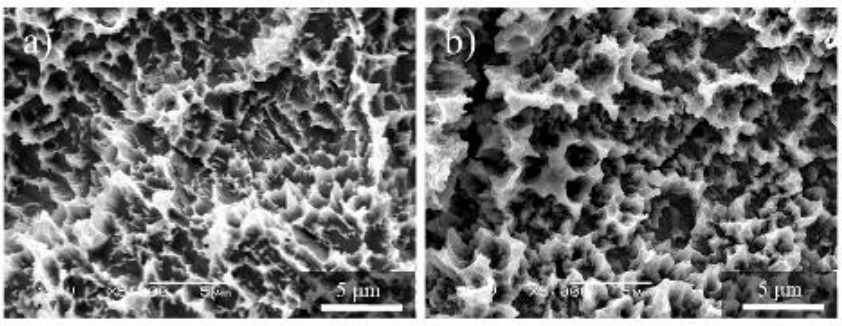

Figure 2. SEM profiles of the surfaces of the (a) Ti and (b) ZrO_2/Ti disks.

Figure 3 shows the AFM profiles of the Ti and ZrO_2/Ti disk surfaces. The obtained three-dimensional structure was almost identical on both surfaces. Moreover, there was no significant difference in the arithmetic average roughness of the three-dimensional surface ($P > 0.05$) (Table 1).

Preprints (www.preprints.org) | NOT PEER-REVIEWED | Posted: 25 May 2022 doi:10.20944/preprints202205.0348.v1

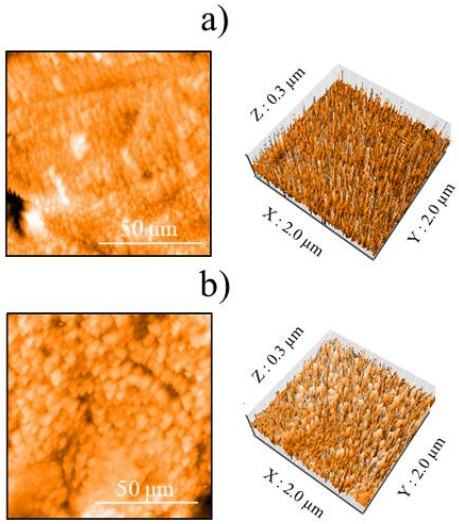

Figure 3. AFM profiles of the surfaces of the (a) Ti and (b) ZrO_2/Ti disks.

Table 1. Three-dimensional surface roughness (Sa) of Ti and ZrO_2/Ti disks

		Square areas			
		10 μm × 10 μm	25 μm × 25 μm	50 μm × 50 μm	100 μm × 100 μm
Sa (μm)	Ti	0.38 (0.12)[a]	0.82 (0.22)[b]	1.11(0.12)[c]	1.30 (0.13)[d]
	ZrO_2/Ti	0.54 (0.19)[a]	0.67 (0.14)[b]	1.05 (0.41)[c]	1.32 (0.03)[d]

Values in brackets are SD.
Same superscripts indicate no significant differences in each square areas between the Ti and ZrO2/Ti groups.

3.1.2. Microstructure and composition of the ZrO_2 coating

Figure 4 shows the EPMA mapping of ZrO_2/Ti disks. The presence of ZrO_2 coating was confirmed by the element mapping of Zr. Cross-sectional observation also identified the presence of Zr in the coating film (arrows in Figure 4b).

Preprints (www.preprints.org) | NOT PEER-REVIEWED | Posted: 25 May 2022 doi:10.20944/preprints202205.0348.v1

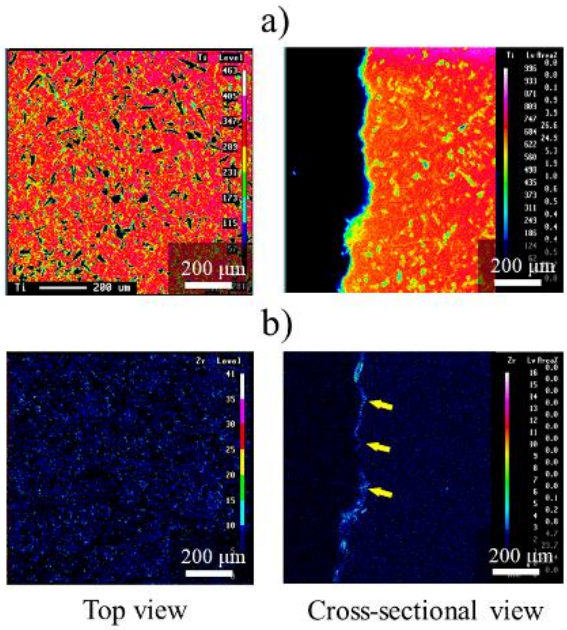

Figure 4. EPMA mappings of ZrO_2/Ti disks. (a) Ti and (b) Zr mappings. The arrows on (b) indicate Zr elements.

Figure 5 shows the XPS results. The O1s peak was observed at 526.5 eV owing to the presence of TiO_2 and ZrO_2. The peaks attributed to $Zr3d_{2/3}$ and $Zr3d_{5/2}$ were observed at 179 and 181 eV, respectively. The peaks of $Ti2p_{3/2}$ and $Ti2p_{1/2}$ of the Ti substrate were observed at 461 and 455 eV, respectively, because of the low thickness of the ZrO_2 layer. Thus, the presence of the ZrO_2 coating on the surface of Ti disks was confirmed.

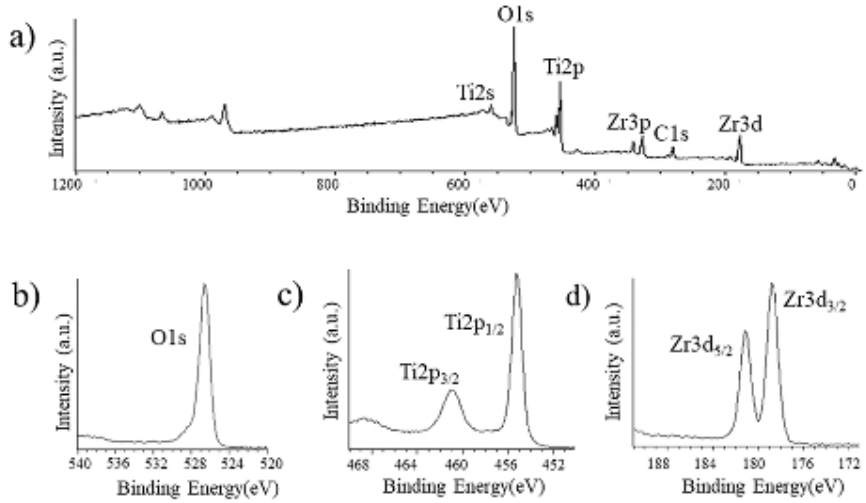

Figure 5. XPS profiles of ZrO_2/Ti disk surfaces. (a) XPS broad spectrum of the ZrO_2/Ti surface. (b) O1s, (c) Ti2p, and (d) Zr3d spectra of ZrO_2/Ti surfaces.

Figure 6 shows the XRD patterns of the ZrO_2 films on the Ti disk. The deposited coating with ZrO_2 structures was confirmed. Corresponding to monoclinic zirconia, a peak was observed at 27.5°, whereas peaks at 36.1°, 37.7°, 41.2°, 54.3°, 62.6°, 69.0°, and 76.7° were observed for tetragonal zirconia. Additionally, Ti peaks were also observed.

Preprints (www.preprints.org) | NOT PEER-REVIEWED | Posted: 25 May 2022 doi:10.20944/preprints202205.0348.v1

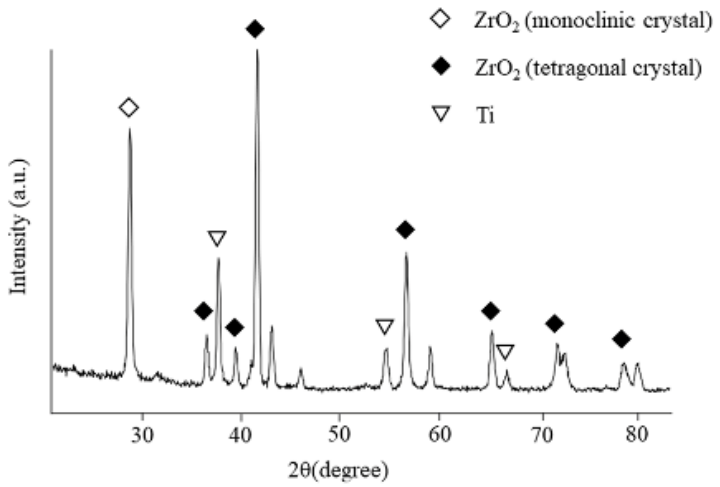

Figure 6. XRD patterns of the films on ZrO_2/Ti disks.

3.1.3. Apparent zeta potential measurements

The apparent zeta potential of ZrO_2/Ti was higher than that of Ti at a pH level of 5.6 (Table 2). Figure 7 shows the pH-dependent curves of the zeta potential at different pH levels. The isoelectric points of Ti and ZrO_2/Ti obtained from Figure 7 are also listed in Table 2. The isoelectric point of ZrO_2/Ti was higher than that of Ti.

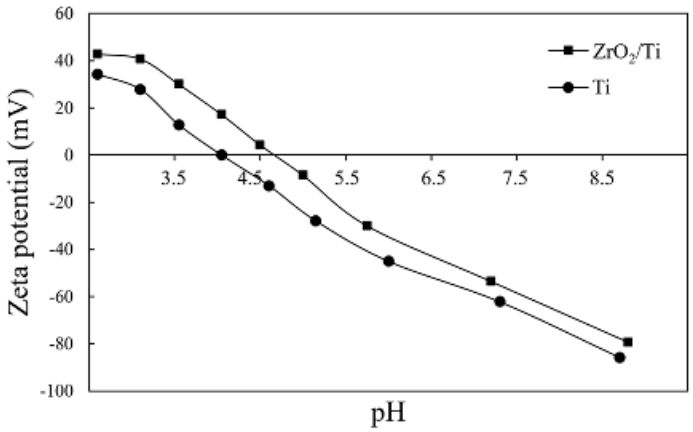

Figure 7. pH-dependent curves of the apparent zeta potentials of Ti and ZrO_2/Ti at any pH level.

Table 2. Apparent zeta potentials at a pH level of 5.6, and the isoelectric points of the Ti and ZrO_2/Ti specimens

Specimen	Zeta potential (mV)	Isoelectric point
Ti	−33.25 (0.08)	4.05
ZrO_2/Ti	−20.69 (0.55)	4.70

Values in brackets are SD.

3.1.4. ZrO_2 coating durability

Figure 8 shows the SEM pictures of the surfaces of ZrO_2/Ti disks after PBS immersion. No differences were observed on the surface morphologies of ZrO_2/Ti disks. The formation of cracks and pinholes was not observed on the surface.

Preprints (www.preprints.org) | NOT PEER-REVIEWED | Posted: 25 May 2022 doi:10.20944/preprints202205.0348.v1

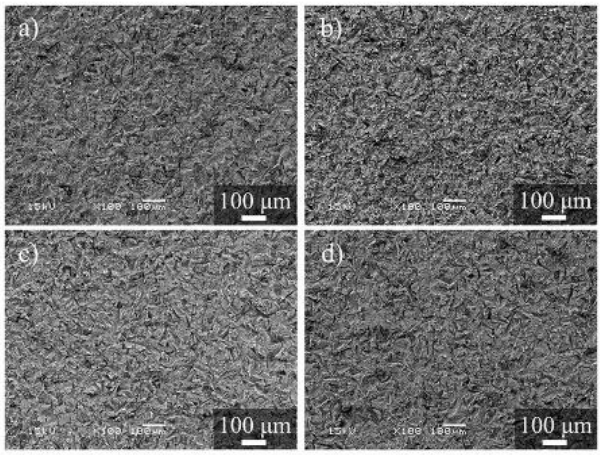

Figure 8. SEM profiles of the surfaces of ZrO_2/Ti disks after PBS immersion. (a) 7, (b) 14, (c) 30, and (d) 90 days after immersion.

3.2. In vitro biocompatibility evaluation (SBF immersion)

Figure 9 shows the SEM images of the surfaces of Ti and ZrO_2/Ti disks after 6 and 24 h of immersion in HBSS. Crystal deposition was observed on all specimen surfaces. However, the growth of crystals was more on the surfaces of ZrO_2/Ti disks compared to that on the surfaces of Ti disks after 6 and 24 h of immersion.

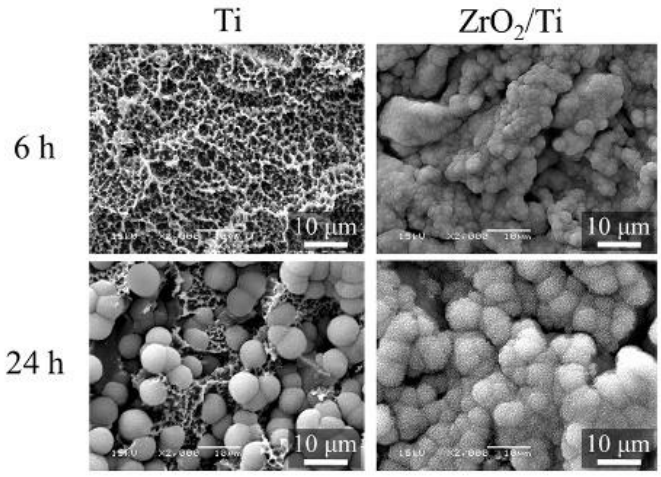

Figure 9. SEM profiles of the surfaces of the Ti and ZrO_2/Ti disks after SBF immersion. (a), (c) Ti and (b), (d) ZrO_2/Ti disks. (a), (b) 6 and (b), (d) 24 h after immersion.

Figure 10 shows the XRD and FT-IR profiles of the precipitated crystals 24 h after immersion. The peaks of the XRD patterns derived from apatite structures were identified at approximately 23.0°, 26.0°, 28.5°, 32.0°, 33.5°, and 46.5°. The peaks of the FT-IR spectra derived from phosphate groups were detected in the ranges of 550–600 and 900–1200 cm^{-1}, whereas those from carbonyl groups were detected at approximately 1200 cm^{-1}. Therefore, the precipitated crystals were identified as carbonate-containing hydroxyapatite.

Preprints (www.preprints.org) | NOT PEER-REVIEWED | Posted: 25 May 2022 doi:10.20944/preprints202205.0348.v1

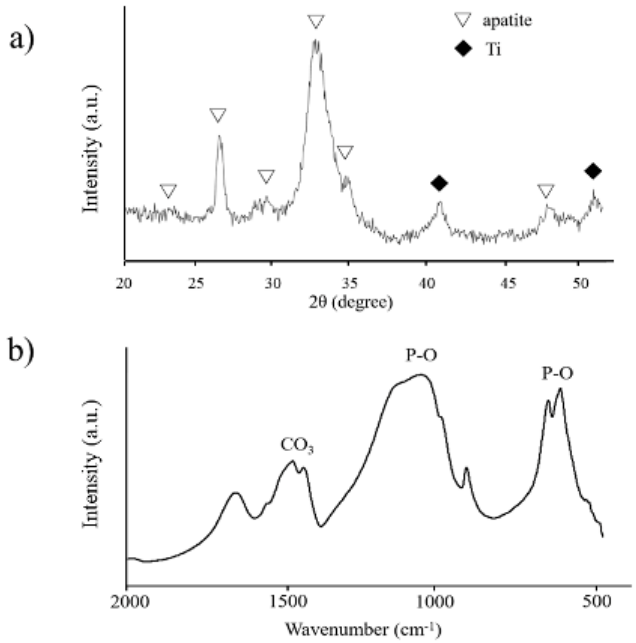

Figure 10. (a) XRD profiles of the deposited crystals on ZrO_2/Ti disks after 14 days of HBSS immersion. (b) FT-IR spectrum of the deposited crystals on ZrO_2/Ti disks after 14 days of HBSS immersion.

3.3. Histological and histomorphometrical evaluations

The rats remained in good health during the experiment. No clinical signs of inflammation or adverse tissue reactions were observed when the animals were sacrificed, and all implants were still in situ.

Figures 11 and 12 show the histological appearances of the ZrO_2/Ti and Ti implants. Permeation of inflammatory cells was not observed. New bone formation was observed around the implants after 2 and 4 weeks of implantation. Bone remodeling proceeded, and mature bone formation was detected. Tight bone-to-implant bonding was observed for the ZrO_2/Ti and Ti implants. However, some gaps were present between the bone and the ZrO_2/Ti and Ti implants. Overall, Ti implants showed more gaps between the bone and the implant surface.

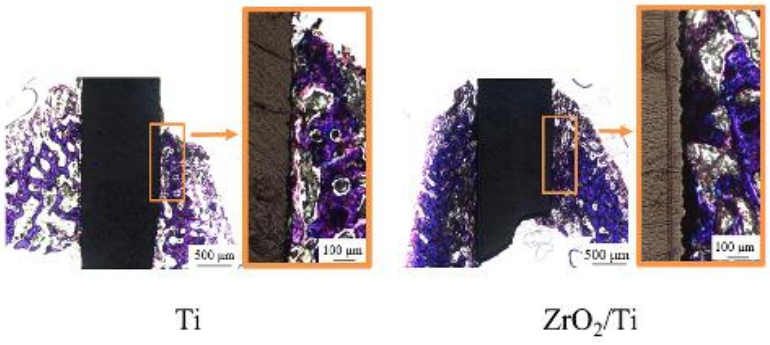

Figure 11. Histological appearances after 2 weeks of implantation into the femur bone defects of rats (magnification of ×40 and ×100).

Preprints (www.preprints.org) | NOT PEER-REVIEWED | Posted: 25 May 2022 doi:10.20944/preprints202205.0348.v1

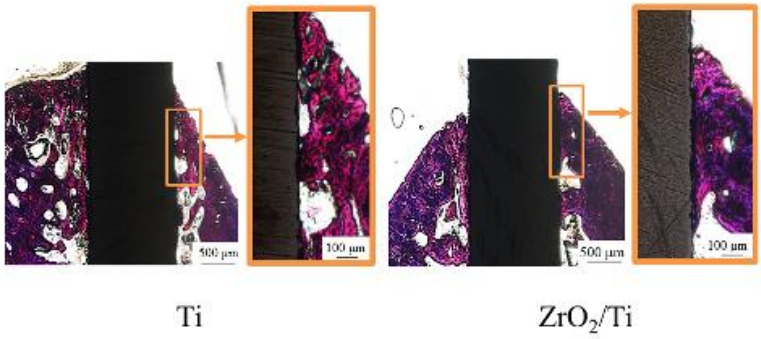

Figure 12. Histological appearances after 4 weeks of implantation into the femur bone defects of rats (magnification of ×40 and ×100).

Table 3 shows the percentages of the BIC ratio and BM values after 2 and 4 weeks of implantation. The BIC ratio and BM values for ZrO_2/Ti implants at 2 weeks were significantly higher than those for Ti implants ($P < 0.05$). At 4 weeks of implantation, there were no significant differences between the Ti and ZrO_2/Ti implants in terms of the BIC ratio and BM values ($P > 0.05$). The BIC ratio and BM values for the Ti implants at 4 weeks were significantly higher than those for Ti implants at 2 weeks ($P < 0.05$). However, no significant differences were observed between the BIC ratio and BM values of ZrO_2/Ti implants after 2 and 4 weeks ($P > 0.05$).

Table 3. Percentage of the measured BIC ratio and BM values

Implantation period	Specimen	BIC ratio (%)	BM (%)
2 weeks	Ti	58.8 (1.33)$^{a, A}$	64.0 (0.69)$^{a, A}$
	ZrO_2/Ti	72.9 (0.70)$^{b, C}$	73.5 (2.31)$^{b, C}$
4 weeks	Ti	72.5 (2.58)$^{c, B}$	71.5 (2.13)$^{c, B}$
	ZrO_2/Ti	73.6 (3.08)$^{c, C}$	72.1 (2.82)$^{c, C}$

Values in brackets are SD.
Same superscripts indicate no significant differences.
Different small letters indicate significant differences between Ti and ZrO_2/Ti in the same implantation period.
Different capital letters indicate significant differences between the values obtained at 2 and 4 weeks in the same specimen.

4. Discussion

In this study, we prepared ZrO_2-coated Ti implants with the same roughened surface topography as that of Ti implants using the molecular precursor method and evaluated the bone response toward ZrO_2 thin films. It was revealed that the ZrO_2 surface with the same roughness and topography as those of Ti promotes osteogenesis equivalent to or better than that of Ti in the early stages of bone formation.

The surface topography analysis of ZrO_2/Ti using SEM and AFM confirmed that the surface appearances and roughness of Ti and ZrO_2/Ti were almost similar. The molecular precursor method can change the surface chemistry without changing the surface

Preprints (www.preprints.org) | NOT PEER-REVIEWED | Posted: 25 May 2022 doi:10.20944/preprints202205.0348.v1

topography. EPMA showed that ZrO_2 films were uniformly observed on all parts of the substrate.

Some studies have been reported on the osseointegration of ZrO_2 dental implants in comparison with that of Ti implants [27–28]. Gahlert et al [29]. investigated the BIC ratio and peri-implant bone density of ZrO_2 implants with a rough acid-etched surface topography and compared it with Ti-SLA implants in the maxilla of pigs. They reported that there was no difference in the bone responses of ZrO_2 implants and Ti-SLA controls. However, an unacceptable difference was observed in the surface topographies of the ZrO_2 and Ti implants using confocal three-dimensional white light microscopy. The Sa values with roughened ZrO_2 implants were higher than those of Ti-SLA implants. Thus, a majority of the studies on bone responses have not focused on the same surface topography between the ZrO_2 and Ti specimens. This present study is the first study comparing the bone responses of the Ti and ZrO_2 implants with almost similar surface roughnesses and topographies.

The XRD patterns of the ZrO_2 films on the Ti disk revealed that the deposited coating comprised monoclinic and tetragonal zirconia. It is well-known that the crystal structure of ZrO_2 changes with temperature. Therefore, a stabilized agent, such as yttria, is often used to stabilize tetragonal zirconia at room temperature. However, the molecular precursor solution did not contain the stabilized agents. The presence of tetragonal zirconia in this study was due to the extreme thinness of the ZrO_2 films. The atoms in ZrO_2 films can easily move at low energies, which might reduce the phase transition temperature. This provided different results from the bulk of ZrO_2.

SBF immersion experiments suggested that the surface property of ZrO_2 promotes osteogenesis equivalent to or better than that of Ti in the early stages of bone formation. This result corresponded with that observed in the animal experiments. SBF immersion experiments were conducted to evaluate the *in vitro* biocompatibility [24], and the results obtained imply the possibility of the *in vivo* bone bioactivity of the material [30]. The thin ZrO_2 films with the same surface topographies as those of Ti implants were expected to enhance bone formation *in vivo*.

The animal study suggested that with the same surface topography as that of Ti implants, ZrO_2 surface exhibited the promotion of new bone formation surrounding the implants. In this study, the apparent zeta potential measurement showed that the value of ZrO_2/Ti was higher than that of Ti at any pH level. It is inferred that the electrostatic repulsion force of ZrO_2 against bone proteins, such as osteocalcin and osteopontin, which are negatively charged, may be smaller than that of Ti. Thus, these reactions may promote bone formation on ZrO_2.

In the animal experiments, implants were inserted into the femurs of rats. The BIC ratio and BM values for ZrO_2/Ti were significantly higher than those of Ti. A significant difference was observed in an especially early stage of bone formation. Albrektsson et al [31]. argued that osseointegration corresponded to approximately 60% bone contact for Ti implants. In this study, the BIC ratio of the Ti implant was 50–70%, whereas that of the ZrO_2/Ti implant was approximately 75%. In other words, the BIC ratio of the ZrO_2/Ti implant was expected to be above the limit prescribed by Albrektsson et al.

This is a new approach to distinguish the effects of surface chemistry from those of surface topography between ZrO_2 and Ti in the osseointegration process. This study is a basic research to evaluate the bone response of the ZrO_2 surface with the same topography as that of Ti for elucidating the osseointegration of ZrO_2 implants. In contrast, it was suggested that ZrO_2-coated Ti implants also have a sufficient clinical value from the viewpoint of BIC ratio and BM value. Non-metallic implants have been reported to exhibit the risks of fracture [32]. Therefore, ZrO_2 is often used as implant abutments only in clinical. However, ZrO_2-coated Ti implants can resolve this fracture problem because of the better mechanical properties of Ti. Moreover, it is expected that a ZrO_2 film preventing corrosion on the Ti substrate will lead to a decrease in allergies and hypersensitivity problems.

According to the results of this study, it is suggested that the ZrO_2 surface with the same surface topography as that of Ti implants can promote bone formation. In other

 doi:10.20944/preprints202205.0348.v1

words, ZrO_2 implant surfaces are required to have the same roughness as that of Ti implants despite the difficulty in processing. Moreover, sandblasting Y-TZP surfaces caused a problem of phase-transformation [33]. Hirota et al. prepared a unique roughened surface of Y-TZP by nano-pulsed laser irradiation without phase-transformation, thereby enhancing the bone response [25]. Thus, it is important to have efficient roughened ZrO_2 surfaces, as those in Ti implants, without phase-transformation to achieve ZrO_2 osseointegration.

5. Conclusions

In this study, we demonstrated the bone response of the ZrO_2 surface with the same roughness and topography as those observed with Ti implants. The molecular precursor method, which can deposit any shape without changing the material surface topography, produced a thin ZrO_2 film on the rough Ti surface. It was revealed that ZrO_2 with the same surface topography as that of roughened Ti implants promoted osteogenesis equivalent to or better than that of Ti in the early stages of bone formation. The osseointegration mechanism will be clarified by investigating the ZrO_2 surface chemistry details.

Author Contributions: Conceptualization, Y.T, M.H and T.H.; methodology, Y.T, M.H and T.H.; validation, Y.T, M.H and T.H.; formal analysis, Y.T.; investigation, Y.T.; data curation, Y.T.; writing—original draft preparation, Y.T, M.H and T.H.; writing—review and editing, M.H. and T.H.; supervision, M.H. and T.H; project administration, T.H.; funding acquisition, T.H. All authors have read and agreed to the published version of the manuscript.

Funding: This work was supported by the Grants-in-Aid for Scientific Research (C) (20K10021) from the Japan Society for the Promotion of Science.

Institutional Review Board Statement: Not applicable.

Informed Consent Statement: Not applicable.

Data Availability Statement: Data presented in this article is available on request from the corresponding author.

Acknowledgments: The authors acknowledge the assistance of Dr. Chihiro Mochizuki in the XRD, and FT-IR analyses. We are grateful to Dr. Mitsunobu Sato and Mr. Hiroki Hara for their valuable advice on the molecular precursor method.

Conflicts of Interest: The authors have no conflicts of interest directly relevant to the content of this article.

References

1. Hanawa, T. Zirconia versus titanium in dentistry: A review. *Dent. Mater. J.* **2020**, 39, 24-36.
2. Siddiqi, A.; Payne, A.G.T.; De Silva, R.K.; Duncan, W.J. Titanium allergy: could it affect dental implant integration? *Clin. Oral. Implants. Res.* **2011**, 22, 673-680.
3. Javed, F.; Al-Hezaimi, K.; Almas, K.; Romanos, G.E. Is titanium sensitivity associated with allergic reactions in patients with dental implants? A systematic review. *Clin. Implant. Dent. Relat. Res.* **2013**, 15, 47-52.
4. Blaschke, C.; Volz, U. Soft and hard tissue response to zirconium dioxide dental implants—a clinical study in man. *Neuro. Endocrinol. Lett.* **2006**, 27, 69-72.
5. Kohal, R.J.; Spies, B.C.; Bauer, A.; Butz, F. One-piece zirconia oral implants for single-tooth replacement: Three-year results from a long-term prospective cohort study. *J. Clin. Periodontol.* **2018**, 45, 114-124.
6. Roehling, S.; Schlegel, K.A.; Woelfler, H.; Gahlert, M. Zirconia compared to titanium dental implants in preclinical studies-A systematic review and meta-analysis. *Clin. Oral. Implants. Res.* **2019**, 30, 365-395.
7. Albrektsson, T.; Wennerberg, A. On osseointegration in relation to implant surfaces. *Clin. Implant. Dent. Relat. Res.* **2019**, 21, 4-7.
8. Wang, Q.; Zhou, P.; Liu, S.; Attarilar, S.; Ma, R.L.; Zhong, Y.; Wang, L. Multi-scale surface treatments of titanium implants for rapid osseointegration: A review. *Nanomaterials.* **2020**, 10, 1244.
9. Khandelwal, N.; Oates, T.W.; Vargas, A.; Alexander, P.P.; Schoolfield, JD.; Alex, McMahan, C. Conventional SLA and chemically modified SLA implants in patients with poorly controlled type 2 diabetes mellitus—a randomized controlled trial. *Clin. Oral. Implants. Res.* **2013**, 24, 13-19.
10. Chiang, H.J.; Hsu, H.J.; Peng, P.W.; Wu, C.Z.; Ou, K.L.; Cheng, H.Y.; Walinski, C.J.; Sugiatno, E. Early bone response to machined, sandblasting acid etching (SLA) and novel surface-functionalization (SLAffinity) titanium implants: characterization, biomechanical analysis and histological evaluation in pigs. *J. Biomed. Mater. Res. A.* **2016**, 104, 397-405.
11. Chambrone, L.; Shibli, J.A.; Mercúrio, C.E.; Cardoso, B.; Preshaw, P.M. Efficacy of standard (SLA) and modified sandblasted and acid-etched (SLActive) dental implants in promoting immediate and/or early occlusal loading protocols: a systematic review of prospective studies. *Clin. Oral. Implants. Res.* **2015**, 26, 359-370.
12. Iinuma, Y.; Hirota, M.; Hayakawa, T.; Ohkubo, C. Surrounding tissue response to surface-treated zirconia implants. *Materials.* **2019**, 13, 30.
13. Zhang, Y.; Lawn, B.R. Novel zirconia materials in dentistry. *J. Dent. Res.* **2018**, 97, 140-147.
14. Bormann, K.H.; Gellrich, N.C.; Kniha, H.; Dard, M.; Wieland, M.; Gahlert, M. Biomechanical evaluation of a microstructured zirconia implant by a removal torque comparison with a standard Ti-SLA implant. *Clin. Oral. Implants. Res.* **2012**, 23, 1210-1216.
15. Sato, M.; Hara, H.; Nishide, T.; Sawada, Y. A water-resistant precursor in a wet process for TiO2 thin film formation. *J. Mater. Chem.* **1996**, 6, 1767-1770.
16. Sato, M.; Hara, H.; Kuritani, H.; Nishide, T. Novel route to Co3O4 thin films on glass substrates via N-alkyl substituted amine salt of Co(III)-EDTA complex. *Sol. Energy. Mater. Sol. Cells.* **1997**, 45, 43-49.
17. Sato, M.; Tanji, T.; Hara, H.; Nishide, T.; Sakashita, Y. SrTiO3 film fabrication and powder synthesis from a non-polymerized. *J. Mater. Chem.* **1999**, 9, 1539-1542.
18. Hayakawa, T.; Sato, M. Molecular precursor method for thin carbonate-containing apatite coating on dental implants. *Dent. Mater. J.* **2020**, 39, 181-186.
19. Takahashi, K.; Hayakawa, T.; Yoshinari, M.; Hara, H.; Mochizuki, C.; Sato, M.; Nemoto, K. Molecular precursor method for thin calcium phosphate coating on titanium. *Thin. Solid. Films.* **2005**, 484, 1-9.
20. Amemiya, T.; Fukayo, Y.; Nakaoka, K.; Hamada, Y.; Hayakawa, T. Tissue response of surface-modified three-dimensional titanium fiber structure. *J. Hard. Tissue. Biol.* **2014**, 23, 137-148.
21. Buser, D.; Broggini, N.; Wieland, M.; Schenk, R.K.; Denzer, A.J.; Cochran, D.L.; Hoffmann, B.; Lussi, A.; Steinemann, S.G. Enhanced bone apposition to a chemically modified SLA titanium surface. *J. Dent. Res.* **2004**, 83, 529-533.
22. Hermina, B.; Thomas, L.; Irena, P. Zeta potential determination of polymeric materials using two differently designed measuring cells of an electrokinetic analyzer. *Acta. Chimica. Slovenica.* **2010**, 57, 700-706.
23. Salgin, S.; Salgin, U.; Soyer, N. Streaming potential measurements of polyethersulfone ultrafiltration membranes to determine salt effects on membrane zeta potential. *Int. J. Electrochem. Sci.* **2013**, 8, 4073-4084.
24. Hanawa, T.; Ota, M. Calcium phosphate naturally formed on titanium in electrolyte solution. *Biomaterials.* **1991**, 12, 767-774.
25. Hirota, M.; Harai, T.; Ishibashi, S.; Mizutani, M.; Hayakawa, T. Cortical bone response toward nanosecond-pulsed laser-treated zirconia implant surfaces. *Dent. Mater. J.* **2019**, 38, 444-451.
26. Yagi, R.; Mochizuki, C.; Sato, M.; Toyama, T.; Hirota, M.; Hayakawa, T.; Ohkubo, C. Characterization and bone response of carbonate-containing apatite-coated titanium implants using an aqueous spray coating. *Materials.* **2017**, 10, 1416.
27. Özkurt, Z.; Kazazoğlu, E. Zirconia dental implants: a literature review. *J. Oral. Implantol.* **2011**, 37, 367-376.
28. Yoshinari, M. Future prospects of zirconia for oral implants -A review. *Dent. Mater. J.* **2020**, 39, 37-45.
29. Gahlert, M.; Roehling, S.; Sprecher, C.M.; Kniha, H.; Milz, S.; Bormann, K. In vivo performance of zirconia and titanium implants: a histomorphometric study in mini pig maxillae. *Clin. Oral. Implants. Res.* **2012**, 23, 281-286.
30. Kokubo, T.; Takadama, H. How useful is SBF in predicting in vivo bone bioactivity? *Biomaterials.* **2006**, 27, 2907-2915.

 doi:10.20944/preprints202205.0348.v1

31. Albrektsson, T.; Eriksson, A.R.; Friberg, B.; Lekholm, U.; Lindahl, L.; Nevins, M.; Oikarinen, V.; Roos, J.; Sennerby, L.; Astrand, P. Histologic investigations on 33 retrieved Nobelpharma implants. *Clin. Mater.* **1993**, 12, 1-9.
32. Kong, N.; Chen, A.; Yan, W.; Zhang, H. Ceramic implant fracture: A clinical report. *J. Prosthet. Dent.* **2019**, 122, 425-429.
33. Bhargava, S.; Doi, H.; Kondo, R.; Aoki, H.; Hanawa, T.; Kasugai, S. Effect of sandblasting on the mechanical properties of Y-TZP zirconia. *Biomed. Mater. Eng.* **2012**, 22, 383-398.